An improved interpolating element-free Galerkin method with nonsingular weight function for two-dimensional potential problems*

Wang Ju-Feng(王聚丰)[a)b)], Sun Feng-Xin(孙凤欣)[a)c)], and Cheng Yu-Min(程玉民)[a)†]

[a)] *Shanghai Institute of Applied Mathematics and Mechanics, Shanghai Key Laboratory of Mechanics in Energy Engineering, Shanghai University, Shanghai* 200072, *China*

[b)] *Ningbo Institute of Technology, Zhejiang University, Ningbo* 315100, *China*

[c)] *Faculty of Science, Ningbo University of Technology, Ningbo* 315016, *China*

(Received 20 February 2012; revised manuscript received 4 March 2012)

In this paper, an improved interpolating moving least-square (IIMLS) method is presented. The shape function of the IIMLS method satisfies the property of Kronecker δ function. The weight function used in the IIMLS method is nonsingular. Then the IIMLS method can overcome the difficulties caused by the singularity of the weight function in the IMLS method. And the number of unknown coefficients in the trial function of the IIMLS method is less than that of the moving least-square (MLS) approximation. Then by combining the IIMLS method with the Galerkin weak form of the potential problem, the improved interpolating element-free Galerkin (IIEFG) method for two-dimensional potential problems is presented. Compared with the conventional element-free Galerkin (EFG) method, the IIEFG method can directly use the essential boundary conditions. Then the IIEFG method has a higher accuracy. For demonstration, three numerical examples are solved using the IIEFG method.

Keywords: meshless method, improved interpolating moving least-square method, improved interpolating element-free Galerkin method, potential problem

PACS: 02.60.Cb, 02.60.Lj, 02.30.Em **DOI:** 10.1088/1674-1056/21/9/090204

1. Introduction

Some traditional numerical methods, such as the finite element method (FEM) and the boundary element method (BEM), are very successful in solving science and engineering problems. However, they cannot be effectively applied to some complicated problems, such as extremely large deformation and crack growth problems. To overcome these limitations, meshless methods have been developed in recent years. The most important common feature of the meshless methods is that the trial function is constructed from a set of nodes with a minimum of or no meshing at all. They show many advantages over the FEM in a class of problems that are not well suited to be studied with the traditional computational methods.[1−4] Based on different approximation functions, many kinds of meshless methods have been proposed.[5]

The moving least-square (MLS) approximation is one of the most important methods to form the shape function in the meshless method. The MLS approximation is developed from the conventional least-square method. In practical numerical process, the MLS approximation is the conventional least-square method for each selected point in the local influence domain. The MLS approximation was first introduced by Shepard[6] for constructing smooth approximations to fit a specified cloud of points. It was then extended by Lancaster and Salkauskas[7] to surface generation problems. The shape function in the MLS approximation is simple, and the meshless method based on the MLS approximation can offer a solution with high accuracy.[8−15]

A disadvantage of the MLS approximation is that the shape function does not satisfy the property of Kronecker δ function. Then the meshless methods based on the MLS approximation cannot be applied with the essential boundary conditions as directly and easily as the FEM.

*Project supported by the National Natural Science Foundation of China (Grant No. 11171208) and the Shanghai Leading Academic Discipline Project, China (Grant No. S30106).

†Corresponding author. E-mail: ymcheng@shu.edu.cn

© 2012 Chinese Physical Society and IOP Publishing Ltd

Lancaster and Salkauskas[7] presented an interpolating moving least-square (IMLS) method based on the MLS approximation with a singular weight function. The shape function of the IMLS method satisfies the property of Kronecker δ function, then the meshless methods based on the IMLS method can be applied with the essential boundary condition directly without any additional numerical effort. Kaljevic and Saigal[16] presented an improved formulation of the element-free Galerkin (EFG) method based on the IMLS method. Ren *et al.*[17,18] revised the formulae of the IMLS method, and presented an interpolating element-free Galerkin method and an interpolating boundary element-free method for two-dimensional potential and elasticity problems, respectively.

A disadvantage of the IMLS method is that the weight function is singular at the nodes. It complicates the computation of the inverse of the singular matrix, and it causes many difficulties in obtaining the derivatives of the approximation function in the IMLS method. The computing speed and efficiency are reduced due to the singularity. To overcome the singularity, Netuzhylov[19] presented a perturbation technique in the IMLS method by using a small positive number ε within the regularized weight function matrix. However, the appropriate value of ε cannot be determined theoretically, and the errors of the approximation function and its derivatives are often influenced by ε.

In this paper, an improved interpolating moving least-square (IIMLS) method with a nonsingular weight function is presented. The shape function of the IIMLS method satisfies the property of Kronecker δ function. Thus the essential boundary condition can be applied directly and easily in the meshless method based on the IIMLS method. The weight function used in the IIMLS method is not singular at any point. Any weight function used in the MLS approximation can be chosen as the weight function in the IIMLS method. Then the IIMLS method can overcome the difficulties caused by the singularity of the weight function in the IMLS method. And the number of the unknown coefficients in the trial function of the IIMLS method is less than that of the MLS approximation. Then we can select fewer nodes in the local influence domain in the IIMLS method, and a higher computational accuracy can be obtained.

Then combining the IIMLS method in this paper with the Galerkin weak form of the potential problem, we present an improved interpolating element-free Galerkin (IIEFG) method for two-dimensional potential problems, and the corresponding formulae are obtained. The essential boundary conditions are applied naturally and directly in the IIEFG method. The IIEFG method gives a greater computational accuracy. Some numerical examples are presented to demonstrate the method.

2. Improved interpolating moving least-square method

Let $p_1(\boldsymbol{x}), p_2(\boldsymbol{x}), \ldots, p_m(\boldsymbol{x})$ be the given basis functions, and $p_1(\boldsymbol{x}) \equiv 1$. In order to let the shape function of the IIMLS method, in which the nonsingular weight function is used, satisfy the property of Kronecker δ function, we first generate a new set of basis functions.

For a given point $\boldsymbol{x} \in \Omega$, let

$$\tilde{p}_i(\bar{\boldsymbol{x}})_x = p_i(\bar{\boldsymbol{x}}) - \sum_{I=1}^{n} v(\boldsymbol{x}, \boldsymbol{x}_I) p_i(\boldsymbol{x}_I), \quad i = 1, 2, \ldots, m, \tag{1}$$

where $\bar{\boldsymbol{x}}$ is the point in the local approximation of $\boldsymbol{x}$, $\boldsymbol{x}_I$ $(I = 1, 2, \ldots, n)$ are the nodes with the domains of influence covering point $\boldsymbol{x}$, and

$$v(\boldsymbol{x}, \boldsymbol{x}_I) = \frac{\zeta(\boldsymbol{x}, \boldsymbol{x}_I)}{\sum\limits_{J=1}^{n} \zeta(\boldsymbol{x}, \boldsymbol{x}_J)}, \tag{2}$$

with

$$\zeta(\boldsymbol{x}, \boldsymbol{x}_I) = \frac{\prod\limits_{J \neq I} ||\boldsymbol{x} - \boldsymbol{x}_J||^2}{\prod\limits_{J \neq I} ||\boldsymbol{x}_I - \boldsymbol{x}_J||^2}. \tag{3}$$

We also need to perform the same transformation of $u(\boldsymbol{x})$. Then let

$$\tilde{u}(\bar{\boldsymbol{x}})_x = u(\bar{\boldsymbol{x}}) - \sum_{I=1}^{n} v(\boldsymbol{x}, \boldsymbol{x}_I) u(\boldsymbol{x}_I). \tag{4}$$

The function $v(\boldsymbol{x}, \boldsymbol{x}_I)$ obviously satisfies

$$v(\boldsymbol{x}_I, \boldsymbol{x}_J) = \delta_{IJ}, \tag{5}$$

and

$$\sum_{I=1}^{n} v(\boldsymbol{x}, \boldsymbol{x}_I) = 1, \quad \forall \boldsymbol{x} \in \Omega. \tag{6}$$

Next we will obtain the approximation function of the new function $\tilde{u}(\bar{\boldsymbol{x}})_x$ by using the MLS approximation with the new basis functions.

Define a local approximation function

$$\tilde{u}_{\mathrm{L}}(\boldsymbol{x},\bar{\boldsymbol{x}})=\sum_{i=1}^{m}\tilde{p}_i(\bar{\boldsymbol{x}})_x\tilde{a}_i(\boldsymbol{x}), \tag{7}$$

where $\tilde{a}_i(\boldsymbol{x})$ are the unknown coefficients of the new basis. From Eqs. (1) and (6), we have

$$\tilde{p}_1(\bar{\boldsymbol{x}})_x=1-\sum_{I=1}^{n}v(\boldsymbol{x},\boldsymbol{x}_I)=0. \tag{8}$$

Then

$$\tilde{u}_{\mathrm{L}}(\boldsymbol{x},\bar{\boldsymbol{x}})=\sum_{i=2}^{m}\tilde{p}_i(\bar{\boldsymbol{x}})_x\tilde{a}_i(\boldsymbol{x}). \tag{9}$$

The $m-1$ coefficients $\tilde{a}_i(\boldsymbol{x})$, $i=2,3,\ldots,m$, can be obtained by using the weighted least-square method.

Then define a functional

$$\begin{aligned}\tilde{J}&=\sum_{I=1}^{n}w(\boldsymbol{x}-\boldsymbol{x}_I)[\tilde{u}_{\mathrm{L}}(\boldsymbol{x},\boldsymbol{x}_I)-\tilde{u}(\boldsymbol{x}_I)_x]^2\\&=\sum_{I=1}^{n}w(\boldsymbol{x}-\boldsymbol{x}_I)\Big[\sum_{I=1}^{n}v(\boldsymbol{x},\boldsymbol{x}_I)u(\boldsymbol{x}_I)\\&\quad+\sum_{i=2}^{m}\tilde{p}_i(\boldsymbol{x}_I)_x\tilde{a}_i(\boldsymbol{x})-u(\boldsymbol{x}_I)\Big]^2.\end{aligned} \tag{10}$$

Equation (10) can be written as

$$\begin{aligned}\tilde{J}=&(\boldsymbol{V}(\boldsymbol{x})\boldsymbol{u}+\tilde{\boldsymbol{P}}(\boldsymbol{x})\tilde{\boldsymbol{a}}(\boldsymbol{x})-\boldsymbol{u})^{\mathrm{T}}\boldsymbol{W}(\boldsymbol{x})(\boldsymbol{V}(\boldsymbol{x})\boldsymbol{u}\\&+\tilde{\boldsymbol{P}}(\boldsymbol{x})\tilde{\boldsymbol{a}}(\boldsymbol{x})-\boldsymbol{u}),\end{aligned} \tag{11}$$

where

$$\tilde{\boldsymbol{a}}^{\mathrm{T}}(\boldsymbol{x})=(\tilde{a}_2(\boldsymbol{x}),\tilde{a}_3(\boldsymbol{x}),\ldots,\tilde{a}_m(\boldsymbol{x})), \tag{12}$$

$$\boldsymbol{u}^{\mathrm{T}}=(u(\boldsymbol{x}_1),u(\boldsymbol{x}_2),\ldots,u(\boldsymbol{x}_n)), \tag{13}$$

$$\boldsymbol{W}(\boldsymbol{x})=\begin{bmatrix}w(\boldsymbol{x}-\boldsymbol{x}_1)&0&\ldots&0\\0&w(\boldsymbol{x}-\boldsymbol{x}_2)&\ldots&0\\\vdots&\vdots&\ddots&\vdots\\0&0&\ldots&w(\boldsymbol{x}-\boldsymbol{x}_n)\end{bmatrix}, \tag{14}$$

$$\tilde{\boldsymbol{P}}(\boldsymbol{x})=\begin{bmatrix}\tilde{p}_2(\boldsymbol{x}_1)_x&\tilde{p}_3(\boldsymbol{x}_1)_x&\ldots&\tilde{p}_m(\boldsymbol{x}_1)_x\\\tilde{p}_2(\boldsymbol{x}_2)_x&\tilde{p}_3(\boldsymbol{x}_2)_x&\ldots&\tilde{p}_m(\boldsymbol{x}_2)_x\\\vdots&\vdots&\ddots&\vdots\\\tilde{p}_2(\boldsymbol{x}_n)_x&\tilde{p}_3(\boldsymbol{x}_n)_x&\ldots&\tilde{p}_m(\boldsymbol{x}_n)_x\end{bmatrix}, \tag{15}$$

and $\boldsymbol{V}(\boldsymbol{x})$ is an $n\times n$ matrix, in which the row is given by

$$\boldsymbol{v}(\boldsymbol{x})=(v(\boldsymbol{x},\boldsymbol{x}_1),v(\boldsymbol{x},\boldsymbol{x}_2),\ldots,v(\boldsymbol{x},\boldsymbol{x}_n)). \tag{16}$$

To obtain $\tilde{a}_i(\boldsymbol{x})$, we let

$$\frac{\partial\tilde{J}}{\partial\tilde{\boldsymbol{a}}}=\tilde{\boldsymbol{A}}(\boldsymbol{x})\tilde{\boldsymbol{a}}(\boldsymbol{x})-\tilde{\boldsymbol{B}}(\boldsymbol{x})\boldsymbol{u}=\boldsymbol{O}, \tag{17}$$

where

$$\tilde{\boldsymbol{A}}(\boldsymbol{x})=\tilde{\boldsymbol{P}}^{\mathrm{T}}(\boldsymbol{x})\boldsymbol{W}(\boldsymbol{x})\tilde{\boldsymbol{P}}(\boldsymbol{x}), \tag{18}$$

$$\tilde{\boldsymbol{B}}(\boldsymbol{x})=\tilde{\boldsymbol{P}}^{\mathrm{T}}(\boldsymbol{x})\boldsymbol{W}(\boldsymbol{x})(\boldsymbol{E}-\boldsymbol{V}(\boldsymbol{x})), \tag{19}$$

and $\boldsymbol{E}$ is an $n\times n$ identity matrix. Thus we have

$$\tilde{\boldsymbol{a}}(\boldsymbol{x})=\tilde{\boldsymbol{A}}^{-1}(\boldsymbol{x})\tilde{\boldsymbol{B}}(\boldsymbol{x})\boldsymbol{u}. \tag{20}$$

Then the local approximation function can be obtained as

$$\begin{aligned}\tilde{\boldsymbol{u}}_{\mathrm{L}}(\boldsymbol{x},\bar{\boldsymbol{x}})&=\sum_{i=2}^{m}\tilde{p}_i(\bar{\boldsymbol{x}})_x\tilde{a}_i(\boldsymbol{x})\\&=\hat{\boldsymbol{p}}(\bar{\boldsymbol{x}})_x\tilde{\boldsymbol{A}}^{-1}(\boldsymbol{x})\tilde{\boldsymbol{B}}(\boldsymbol{x})\boldsymbol{u},\end{aligned} \tag{21}$$

where

$$\hat{\boldsymbol{p}}(\bar{\boldsymbol{x}})_x=(\tilde{p}_2(\bar{\boldsymbol{x}})_x,\tilde{p}_3(\bar{\boldsymbol{x}})_x,\ldots,\tilde{p}_m(\bar{\boldsymbol{x}})_x). \tag{22}$$

From Eqs. (4) and (21), the global interpolating approximation function of $u(\boldsymbol{x})$ is obtained as

$$\tilde{u}^{\mathrm{h}}(\boldsymbol{x})=\tilde{\boldsymbol{\Phi}}(\boldsymbol{x})\boldsymbol{u}=\sum_{I=1}^{n}\tilde{\Phi}_I(\boldsymbol{x})u(\boldsymbol{x}_I), \tag{23}$$

where $\tilde{\boldsymbol{\Phi}}(\boldsymbol{x})$ is a matrix of the shape function

$$\begin{aligned}\tilde{\boldsymbol{\Phi}}(\boldsymbol{x})&=(\tilde{\Phi}_1(\boldsymbol{x}),\tilde{\Phi}_2(\boldsymbol{x}),\ldots,\tilde{\Phi}_n(\boldsymbol{x}))\\&=\boldsymbol{v}(\boldsymbol{x})+\tilde{\boldsymbol{p}}^{\mathrm{T}}(\boldsymbol{x})\tilde{\boldsymbol{A}}^{-1}(\boldsymbol{x})\tilde{\boldsymbol{B}}(\boldsymbol{x}),\end{aligned} \tag{24}$$

and

$$\tilde{\boldsymbol{p}}^{\mathrm{T}}(\boldsymbol{x})=(g_2(\boldsymbol{x}),g_3(\boldsymbol{x}),\ldots,g_m(\boldsymbol{x})), \tag{25}$$

$$g_i(\boldsymbol{x})=p_i(\boldsymbol{x})-\sum_{I=1}^{n}v(\boldsymbol{x},\boldsymbol{x}_I)p_i(\boldsymbol{x}_I). \tag{26}$$

Equation (24) is the shape function of the IIMLS method, and then the IIMLS method is presented.

Obviously, the approximation function in Eq. (23) satisfies the interpolating property, i.e.,

$$\tilde{u}^{\mathrm{h}}(\boldsymbol{x}_I)=u(\boldsymbol{x}_I). \tag{27}$$

And the linear combination of the basis functions can be exactly reproduced by the IIMLS method, i.e., for

$$u(\boldsymbol{x})=\beta_1p_1(\boldsymbol{x})+\beta_2p_2(\boldsymbol{x})+\ldots+\beta_mp_m(\boldsymbol{x}), \tag{28}$$

where $\beta_1,\beta_2,\ldots,\beta_m$ are arbitrary constants, there exists

$$\tilde{u}^{\mathrm{h}}(\boldsymbol{x})=u(\boldsymbol{x}). \tag{29}$$

The shape function of the IIMLS method can satisfy the property of Kronecker δ function. Compared with the IMLS method presented by Lancaster and Salkauskas,[7] the IIMLS method possesses a nonsingular weight function. Then any weight function used in the MLS approximation can also be used in the IIMLS method.

From Eq. (9), it can be seen that the number of the unknown coefficients in the trial function of the IIMLS method is less than that in the trial function of the MLS approximation. Therefore, we can select fewer nodes in the meshless method based on the IIMLS method compared to that based on the MLS approximation.

3. Improved interpolating element-free Galerkin method for potential problems

In this section, the IIEFG method based on the IIMLS method will be presented for two-dimensional potential problems. The advantage of the IIEFG method is that the essential boundary conditions can be applied directly and easily.

Consider the following two-dimensional Poisson's equation:

$$\boldsymbol{\nabla}^2 u(\boldsymbol{x}) + b(\boldsymbol{x}) = 0, \quad \boldsymbol{x} = (x, y) \in \Omega, \tag{30}$$

with boundary conditions of the Dirichlet type

$$u(\boldsymbol{x}) = \bar{u}(\boldsymbol{x}), \quad \boldsymbol{x} \in \Gamma_u, \tag{31}$$

or of the Neumann type

$$q(\boldsymbol{x}) = \frac{\partial u(\boldsymbol{x})}{\partial \boldsymbol{n}} = \bar{q}(\boldsymbol{x}), \quad \boldsymbol{x} \in \Gamma_q, \tag{32}$$

where $u(\boldsymbol{x})$ is an unknown function, $b(\boldsymbol{x})$ is a known function, $\boldsymbol{n}$ is the unit outward vector normal to the boundary Γ, and $\bar{u}$ and $\bar{q}$ are the prescribed values of function $u(\boldsymbol{x})$ and its normal derivative over the boundary Γ, respectively. Notice that $\Gamma = \Gamma_u \cup \Gamma_q$.

The Galerkin weak form of Eqs. (30)–(32) is

$$\int_{\Gamma_q} \delta u \cdot \bar{q}(\boldsymbol{x}) \mathrm{d}\Gamma - \int_{\Omega} \delta(\boldsymbol{\nabla} u)^{\mathrm{T}} \cdot \boldsymbol{\nabla} u \mathrm{d}\Omega + \int_{\Omega} \delta u \cdot b(\boldsymbol{x}) \mathrm{d}\Omega = 0, \tag{33}$$

where

$$\boldsymbol{\nabla} u = \left(\frac{\partial u}{\partial x}, \frac{\partial u}{\partial y} \right)^{\mathrm{T}} = (u_{,x}, u_{,y})^{\mathrm{T}}. \tag{34}$$

We employ n_{t} nodes in domain Ω, and the union of its compact support domains Ω_I, $I = 1, 2, \ldots, n_{\mathrm{t}}$, must cover the whole domain Ω. According to the IIMLS method, the unknown potential $u(\boldsymbol{x})$ at any field point $\boldsymbol{x}$ in domain Ω can be expressed as

$$u(\boldsymbol{x}) = \tilde{\boldsymbol{\Phi}}^{\mathrm{T}}(\boldsymbol{x}) \boldsymbol{u} = \sum_{I=1}^{n} \tilde{\boldsymbol{\Phi}}_I(\boldsymbol{x}) u(\boldsymbol{x}_I), \tag{35}$$

where n is the number of nodes whose compact support domains cover point $\boldsymbol{x}$. Then we have

$$\boldsymbol{\nabla} u = \boldsymbol{\nabla} \tilde{\boldsymbol{\Phi}}^{\mathrm{T}}(\boldsymbol{x}) \boldsymbol{u} = \boldsymbol{B}^{\mathrm{T}} \boldsymbol{u}, \tag{36}$$

where

$$\boldsymbol{B}^{\mathrm{T}} = \begin{bmatrix} \tilde{\Phi}_{1,x}(\boldsymbol{x}) & \tilde{\Phi}_{2,x}(\boldsymbol{x}) & \cdots & \tilde{\Phi}_{n,x}(\boldsymbol{x}) \\ \tilde{\Phi}_{1,y}(\boldsymbol{x}) & \tilde{\Phi}_{2,y}(\boldsymbol{x}) & \cdots & \tilde{\Phi}_{n,y}(\boldsymbol{x}) \end{bmatrix}. \tag{37}$$

Substituting Eq. (35) into Eq. (33) yields

$$\int_{\Gamma_q} \delta \boldsymbol{u}^{\mathrm{T}} \tilde{\boldsymbol{\Phi}}(\boldsymbol{x}) \cdot \bar{q}(\boldsymbol{x}) \mathrm{d}\Gamma - \int_{\Omega} \delta \boldsymbol{u}^{\mathrm{T}} (\boldsymbol{B}\boldsymbol{B}^{\mathrm{T}}) \boldsymbol{u} \mathrm{d}\Omega + \int_{\Omega} \delta \boldsymbol{u}^{\mathrm{T}} \tilde{\boldsymbol{\Phi}}(\boldsymbol{x}) \cdot b(\boldsymbol{x}) \mathrm{d}\Omega = 0. \tag{38}$$

Then we have

$$\delta \boldsymbol{u}^{\mathrm{T}} \left[\int_{\Gamma_q} \tilde{\boldsymbol{\Phi}}(\boldsymbol{x}) \cdot \bar{q}(\boldsymbol{x}) \mathrm{d}\Gamma - \int_{\Omega} \boldsymbol{B}\boldsymbol{B}^{\mathrm{T}} \boldsymbol{u} \mathrm{d}\Omega + \int_{\Omega} \tilde{\boldsymbol{\Phi}}(\boldsymbol{x}) b(\boldsymbol{x}) \mathrm{d}\Omega \right] = 0. \tag{39}$$

Because the nodal test function $\delta \boldsymbol{u}$ is arbitrary, the final discretized equation is obtained as

$$\int_{\Gamma_q} \tilde{\boldsymbol{\Phi}}(\boldsymbol{x}) \cdot \bar{q}(\boldsymbol{x}) \mathrm{d}\Gamma - \int_{\Omega} \boldsymbol{B}\boldsymbol{B}^{\mathrm{T}} \boldsymbol{u} \mathrm{d}\Omega + \int_{\Omega} \tilde{\boldsymbol{\Phi}}(\boldsymbol{x}) b(\boldsymbol{x}) \mathrm{d}\Omega = 0, \tag{40}$$

i.e.,

$$\boldsymbol{K}\boldsymbol{u} = \boldsymbol{F}, \tag{41}$$

where

$$K_{IJ} = \int_{\Omega} \boldsymbol{\nabla} \tilde{\Phi}_I^{\mathrm{T}} \cdot \boldsymbol{\nabla} \tilde{\Phi}_J \mathrm{d}\Omega, \tag{42}$$

$$F_I = \int_{\Gamma_q} \tilde{\Phi}_I \bar{q}(\boldsymbol{x}) \mathrm{d}\Gamma + \int_{\Omega} \tilde{\Phi}_I b(\boldsymbol{x}) \mathrm{d}\Omega. \tag{43}$$

Since the shape function of the IIMLS method satisfies the property of Kronecker δ function, the essential boundary conditions can be applied directly. And then by substituting the boundary conditions of Eq. (31) into Eq. (41), we can obtain the unknowns at nodes by solving the linear equation (41). Thus the IIEFG method is presented for two-dimensional potential problems.

4. Numerical examples

In this section, we will present some numerical examples to show the accuracy of the IIEFG method proposed in this paper. The discrete absolute error e_I is defined as

$$e_I = |u_I - u_I^{\rm h}|, \tag{44}$$

where u_I and $u_I^{\rm h}$ are the analytical and the numerical solutions at $\boldsymbol{x}_I$, respectively.

The weight function plays an important role in the IIMLS method. Compared with the IMLS method, the nonsingular weight function is used in the IIMLS method. Then the cubic spline weight function, i.e.,

$$\begin{aligned} & w(\boldsymbol{x}-\boldsymbol{x}_I) \equiv w(r) \\ & = \begin{cases} 2/3 - 4r^2 + 4r^3, & r \le 1/2, \\ 4/3 - 4r + 4r^2 - 4r^3/3, & 1/2 < r \le 1, \\ 0, & r > 1, \end{cases} \end{aligned} \tag{45}$$

is used in the present analysis. Here

$$r = \frac{d_I}{\rho_I}, \quad d_I = ||\boldsymbol{x} - \boldsymbol{x}_I||, \tag{46}$$

and ρ_I is the radius of the influence domain of node $\boldsymbol{x}_I$.

Example 1 Consider an internal potential problem, in which the warping function $u(x, y)$ is regarded as a part of the torsion problem for an elliptical cross-section $\frac{x^2}{a^2} + \frac{y^2}{b^2} = 1$ with $a = 2$ and $b = 1$.[20] The warping function satisfies the Laplace's equation

$$\boldsymbol{\nabla}^2 u = 0. \tag{47}$$

The analytical solution of this problem is

$$u(x, y) = \frac{(b^2 - a^2)xy}{a^2 + b^2}. \tag{48}$$

The boundary condition is of the Dirichlet type extracted from the above analytical solution.

Due to the symmetry of the model, only a quarter of the problem domain is analysed. The quadratic basis function is used. The cubic spline function (45) is selected as the weight function. We use $\rho_I = 0.8$ and a total of 33 nodes in the problem domain, as shown in Fig. 1. The numerical and the analytical solutions of the warping function along the line $\overline{AB}$ are shown in Fig. 2. It is evident that the numerical results are in excellent agreement with the analytical solutions.

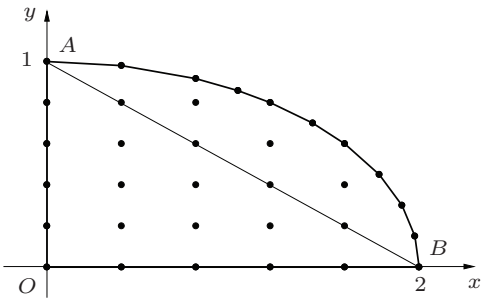


Fig. 1. Node distribution.

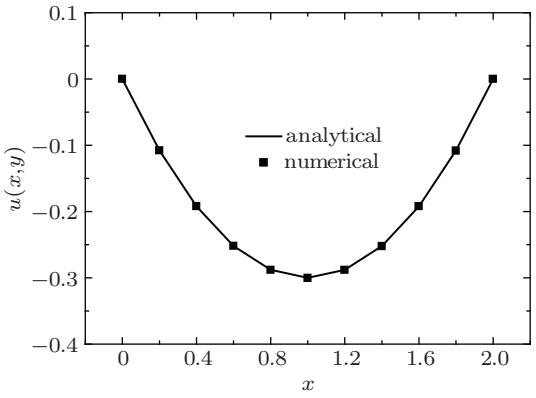


Fig. 2. Analytical and numerical solutions of $u(x, y)$ along line $\overline{AB}$.

When the node distribution in Fig. 1 is used, the absolute errors between the analytical solutions and the numerical ones obtained with the IIEFG and the EFG methods at the inner nodes are shown in Fig. 3. When the node distribution in Fig. 4 is used, the corresponding absolute errors are shown in Fig. 5. Evidently, compared with the conventional EFG method, the IIEFG method improves the computational accuracy.

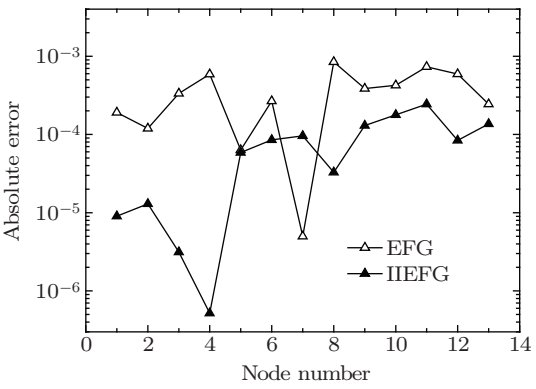


Fig. 3. Absolute errors of the IIEFG and the EFG methods at the inner nodes.

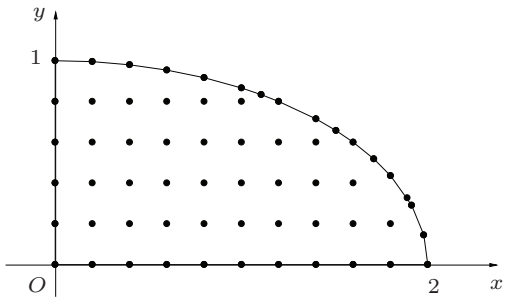


Fig. 4. Node distribution.

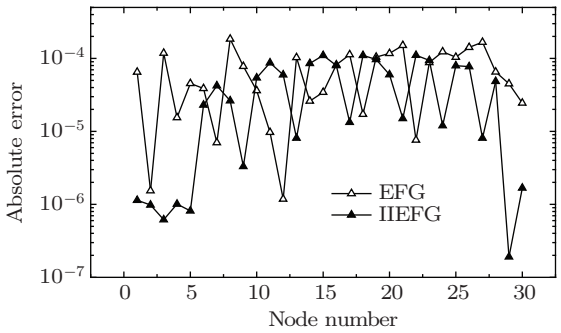


Fig. 5. Absolute errors of the IIEFG and the EFG methods at the inner nodes.

Example 2 Consider a temperature field in a rectangular plate with boundary Γ, which is governed by the Poisson's equation

$$\nabla^2 T(x,y) = -2(x + y - x^2 - y^2), \quad 0 < x < 1, 0 < y < 1. \tag{49}$$

And the boundary condition is

$$T(x, y) = 0, \quad (x, y) \in \Gamma. \tag{50}$$

The analytical solution of this problem is

$$T(x, y) = (x - x^2)(y - y^2). \tag{51}$$

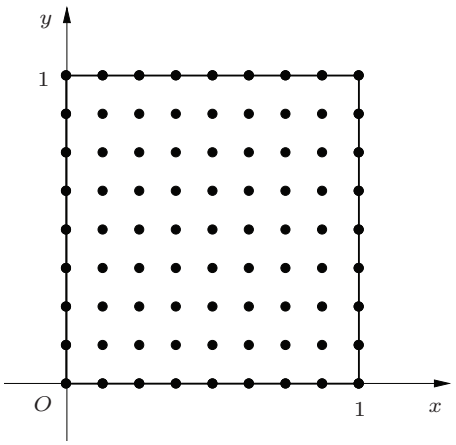


Fig. 6. Node distribution.

The linear basis function is used in this example. A total of 81 nodes are employed on the problem domain (see Fig. 6), and $\rho_I = 0.1375$. Then the numerical and the analytical solutions at $x = 0.5$, 0.375, and 0.25 are shown in Fig. 7. It is also evident that the numerical results are in excellent agreement with the analytical solutions. The absolute errors at the inner nodes with the IIEFG and the EFG methods are shown in Fig. 8. It can be seen that the IIEFG method still has a higher computational accuracy.

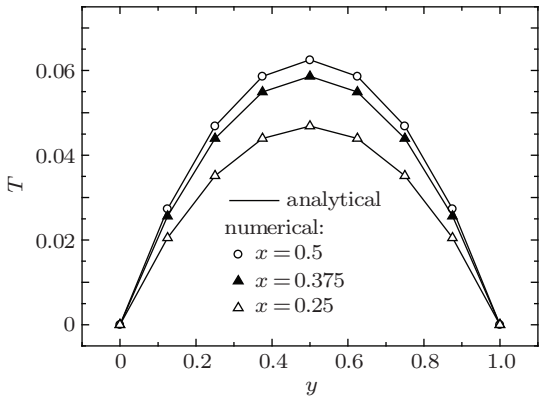


Fig. 7. Analytical and numerical solutions at $x = 0.5$, 0.375, and 0.25.

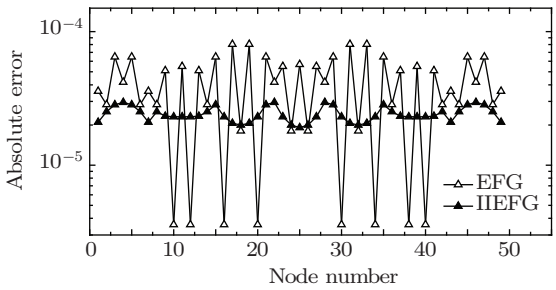


Fig. 8. Absolute errors of the IIEFG and the EFG methods at the inner nodes.

Example 3 Consider a two-dimensional Laplace's equation

$$\nabla^2 T(x,y) = 0, \quad (x,y) \in \Omega, \tag{52}$$

where the domain Ω is shown in Fig. 9.

The analytical solution of this problem is

$$T(x, y) = \mathrm{e}^x \sin y. \tag{53}$$

The boundary condition is of the Dirichlet type extracted from the above analytical solution.

The linear basis function is also used in this example. As shown in Fig. 9, 44 nodes are used for this example, and $\rho_I = 0.3767$. The numerical and the analytical results along the line $\overline{OA}$ are shown in Fig. 10. It is evident that the present numerical results are in excellent agreement with the analytical solutions with

high accuracy. For comparison between the EFG and the IIEFG methods, the absolute errors at the inner nodes are shown in Fig. 11. It still can be seen that the IIEFG method has a higher computational accuracy.

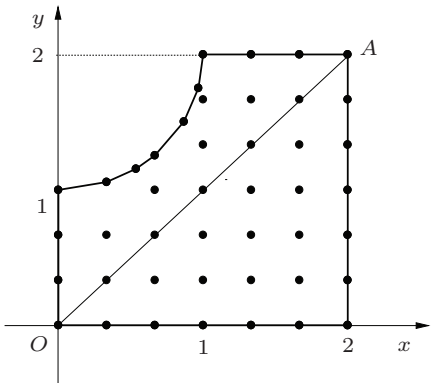


Fig. 9. Node distribution.

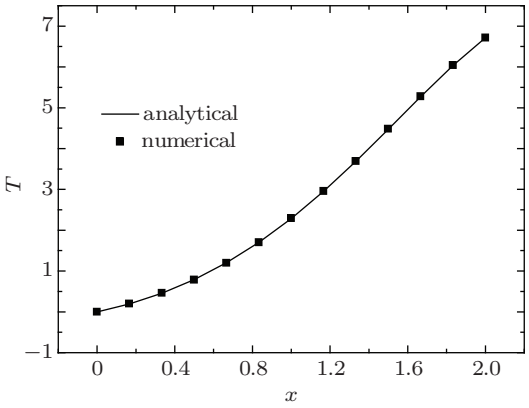


Fig. 10. Analytical and numerical solutions of T along line $\overline{OA}$.

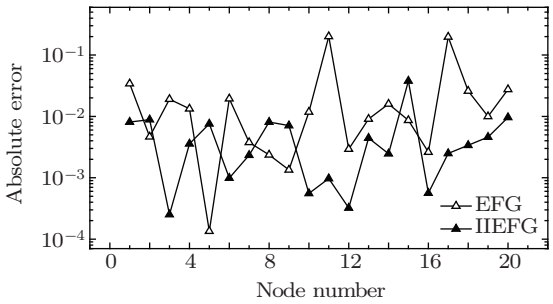


Fig. 11. Absolute errors of the IIEFG and the EFG methods at the inner nodes.

5. Conclusion

In this paper, based on the MLS approximation, the IIMLS method is presented. The shape function of the IIMLS method satisfies the property of Kronecker δ function. And the number of unknown coefficients in the trial function of the IIMLS method is less than that in the trial function of the MLS approximation. The essential boundary condition can be applied directly and easily in the meshless method based on the IIMLS method, and fewer nodes are needed in the local influence domain.

The weight function used in the IIMLS method is nonsingular compared with that in the IMLS method presented by Lancaster and Salkauskas. Then IIMLS method can overcome the difficulty caused by the singularity of the weight function in the IMLS method. Therefore, the IIMLS method has a high computational accuracy.

By combining the IIMLS method in this paper with the Galerkin weak form of the potential problem, the IIEFG method is presented for two-dimensional potential problems, and the corresponding formulae are obtained. Compared with the conventional EFG method, the IIEFG method can naturally and directly use the essential boundary conditions. The IIEFG method gives a higher computational accuracy.

References

[1] Li S C and Cheng Y 2005 *Theoretical and Applied Fracture Mechanics* **44** 234
[2] Liew K M, Ren J and Reddy J N 2005 *International Journal for Numerical Methods in Engineering* **63** 1014
[3] Liew K M, Cheng Y and Kitipornchai S 2005 *International Journal for Numerical Methods in Engineering* **64** 1610
[4] Chen L and Cheng Y 2010 *Chin. Phys.* B **19** 090204
[5] Belytschko T, Krongauz Y, Organ D, Fleming M and Krysl P 1996 *Computer Methods in Applied Mechanics and Engineering* **139** 3
[6] Shepard D 1968 *Proceeding of the 23rd ACM National Conference* (New York: ACM) p. 517
[7] Lancaster P and Salkauskas K 1981 *Mathematics of Computation* **37** 141
[8] Belytschko T, Lu Y Y and Gu L 1994 *International Journal for Numerical Methods in Engineering* **37** 229
[9] Wang J, Sun F and Cheng R 2010 *Chin. Phys.* B **19** 060201
[10] Cheng R and Cheng Y 2007 *Acta Phys. Sin.* **56** 5569 (in Chinese)
[11] Wang J, Bai F and Cheng Y 2011 *Chin. Phys.* B **20** 030206
[12] Cheng Y, Peng M and Li J 2005 *Chinese Journal of Theoretical and Applied Mechanics* **37** 719
[13] Ge H, Liu Y and Cheng R 2012 *Chin. Phys.* B **21** 010206
[14] Liew K M, Cheng Y and Kitipornchai S 2006 *International Journal for Numerical Methods in Engineering* **65** 1310
[15] Liew K M, Cheng Y and Kitipornchai S 2007 *International Journal of Solids and Structures* **44** 4220
[16] Kaljevic I and Saigal S 1997 *International Journal for Numerical Methods in Engineering* **40** 2953
[17] Ren H, Cheng Y and Zhang W 2009 *Chin. Phys.* B **18** 4065
[18] Ren H, Cheng Y and Zhang W 2010 *Science in China Series* G: *Physics Mechanics and Astronomy* **53** 758
[19] Netuzhylov H 2008 *Engineering Analysis with Boundary Elements* **32** 512
[20] Friedrich J 2002 *Computers & Geosciences* **28** 679